Available online at www.sciencedirect.com
SCIENCE DIRECT®
International Journal of Mass Spectrometry 240 (2005) 121–137
International Journal of Mass Spectrometry
www.elsevier.com/locate/ijms

Competitive reactions and diastereoselective C–H bond activation in the McLafferty rearrangement of photoionized 3-methyl valeramide

Jessica Loos[a], Detlef Schröder[a,*], Helmut Schwarz[a,*], Roland Thissen[b], Odile Dutuit[b]

[a] *Institut für Chemie der Technischen Universität Berlin, Straße des 17, Juni 135, 10623 Berlin, Germany*
[b] *Laboratoire de Chimie Physique, Université Paris-Sud, Bât. 350, 91405 Orsay, France*

Received 24 September 2004; accepted 7 October 2004
Available online 19 November 2004

Abstract

Dissociative photoionization of 3-methyl valeramide is characterized by various degradations of the alkyl backbone, initiated by competitive intramolecular hydrogen migrations. The dominating pathway corresponds to butene elimination via the McLafferty rearrangement. At photon energies ($E_{h\nu}$) close to the ionization threshold, the McLafferty rearrangement is followed by a second hydrogen transfer, known as [McLafferty + 1] reaction. The methyl group at C(3) in combination with diastereospecific labeling at C(4) permits steric differentiation of the two γ-H(D)-atoms at C(4) according to the relative orientations of the stereogenic centers. Investigation of the *syn*- and *anti*-[4-D_1]-diastereomers shows a strong preference for activation of the *anti*-γ-hydrogen in the McLafferty rearrangement. A straightforward analysis of the product distribution is impossible, because also C(4′) allows for a [1,5]-H shift, and the contributions of both sites are additionally superimposed by [McLafferty + 1] products. Photoionization studies of six isotopomers, employing tunable synchrotron radiation, combined with kinetic modeling enable a deconvolution of the branching ratios and a determination of the corresponding steric and kinetic isotope effects operative in the McLafferty rearrangement. The kinetic isotope effects (KIEs) are more or less independent of $E_{h\nu}$. The initiating [1,5]-H shifts feature very low KIEs, especially for the C(4)─H bond activation, whereas the subsequent hydrogen atom transfers in the course of the [McLafferty + 1] processes are affected by substantial KIEs. Interestingly, the steric effect (SE) decreases considerably at low $E_{h\nu}$ (SE = 1.8, 2.6, and 2.8 at $E_{h\nu}$ = 9.6, 10, and 11 eV, respectively), which can be explained by more pronounced epimerization prior to dissociation at lower energies.

Keywords: C─H activation; Distonic ions; Ion-neutral complexes; Isotope effects; Mass spectrometry; Steric effects

1. Introduction

The McLafferty rearrangement [1,2] is arguably the most prominent and one of the best studied fragmentation processes of ionized carbonyl compounds and intrigues by its high regiospecificity. Especially for amides the selectivity is remarkable, since here the McLafferty reaction is not subject to the same extensive H-rearrangements as has been observed for structurally comparable carboxylic acids and esters [3]. The stereospecific aspects of this important reaction, however, have mainly been studied for rigid or cyclic systems where it can be considerable [4]; examples for flexible systems [5–7] are rare and display rather small stereoselective effects. Nevertheless, steric effects (SEs) can provide important mechanistic information complementary to that obtained from the analysis of kinetic isotope effects (KIEs). Thus, while the KIEs depend on the intrinsic structural details of the key step of bond activation (here, the γ-C–H bond activation), the SEs reflect conformational constraints induced by the backbone of the substrate [8].

In order to obtain a deeper understanding of the diastereoselectivity of the McLafferty rearrangement in a flexible aliphatic carbonyl compound such as valeramide, a steric marker is introduced in the carbon backbone in the vicinity to the (secondary) γ-C-atom, such that diastereospecific

* Corresponding authors. Tel.: +49 30 314 26546 (D. Schröder)/+49 30 314 23483 (H. Schwarz); fax: +49 30 314 21102.
E-mail addresses: detlef.schroeder@mail.chem.tu-berlin.de (D. Schröder), helmut.schwarz@mail.chem.tu-berlin.de (H. Schwarz).

1387-3806/$ – see front matter © 2004 Elsevier B.V. All rights reserved.
doi:10.1016/j.ijms.2004.10.010

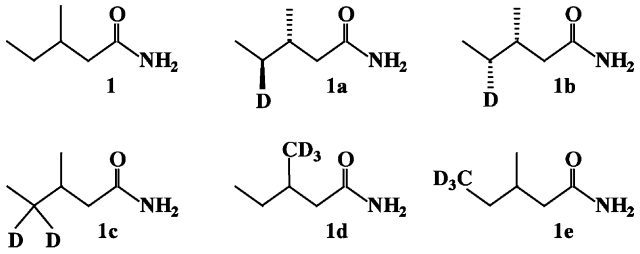

Plate 1.

[D_1]-labeling of the γ-position then allows to monitor any difference between the McLafferty reaction involving one or the other of the two possible, now diastereotopic H(D) atoms. The particular aptitude of a system closely related to valeramide lays in the high regioselectivity of the McLafferty reaction of amides, which is a major advantage for an "unperturbed" investigation of stereochemical effects. Moreover, valeramide itself is the simplest system with secondary γ-hydrogens, and may thus serve as a model for larger carboxamides [9]. Last but not least, extensive experimental and computational studies of ionized valeramide [10–13] provide a solid base of knowledge about the parent system. As the general fragmentation pattern of the alkylated system has to be kept comparable to that of valeramide, the steric marker at the stereogenic center should neither be too bulky nor cause substantial differences in reactivity. We thus chose 3-methyl valeramide (**1**), because a methyl group fulfils best these demands on the steric marker. In addition to the unlabeled compound, five deuterated isotopomers (**1a**–**e**) have been examined to follow the regio- and stereochemistry (Plate 1).

2. Methods

All experiments were performed with the CERISES [14] apparatus, mounted to the beam-line SA63 of the synchrotron SuperACO at LURE (Orsay, France). The line includes a normal incidence monochromator which provides tunable VUV-light in the range of 7–35 eV. Slits were opened to 1 mm, corresponding to a photon-energy resolution of about 500 (i.e., 20 meV at 10 eV). The accuracy of the photon energy ($E_{h\nu}$) was verified by measuring the ionization threshold of argon within 2 meV of its nominal value. Unless stated otherwise, a lithium-fluoride window was inserted at $E_{h\nu} \leq 11.8$ eV to effectively eliminate higher-order photons emerging from the grating of the monochromator. Experiments without LiF filter are inherently interfered by higher-order photons and are reported without corrections. Neutral 3-methyl valeramide and its isotopomers were introduced into the source either via a 0.5 m long gas-line (stainless steel) or, after upgrading of the instrument, via a regular solid probe. Note that introduction of the substrate through the gas-line causes substantial memory effects. After ionization by monochromatic photons, the formed electrons and cations are extracted in opposite directions from the source by a small electrostatic field of 1 V/cm. In the present experiments, electrons of low kinetic energies were detected without detailed velocity analysis, and the cations were transferred into a QOQ system[1] (Q stands for quadrupole and O for octopole). The product ions were analyzed by Q2 and detected by a multi-channel plate operating in the counting mode. For each isotopomer overview mass-spectra were recorded at selected energies, before scanning the McLafferty-product region (m/z = 59–62) with increased mass resolution at $E_{h\nu}$ = 9.6, 10, and 11 eV, respectively. Appearance energies (AEs) of relevant fragment ions were determined in single-ion monitoring mode while scanning $E_{h\nu}$, and derived by linear extrapolation of the onsets to the baseline without applying any further corrections for temperature, kinetic shifts, etc. The ionization energy (IE) of the parent molecule was retrieved as the first point with a notable ion signal. Note that the excitation as well as the mass spectra were not taken in the coincidence mode (TPEPICO) and that the parent ions therefore were generated with an energy distribution $E_{\text{internal}} \leq (E_{h\nu} - \text{IE}) - E_{\text{electron}}$.

The synthesis of the labeled (>98 atom.% D) 3-methyl valeramides[2] followed previously described strategies [15,16]. Briefly, the amides were made by ammonolysis of the corresponding esters or acid chlorides. The 3-methylvaleric acids for the synthesis of **1c**–**e** were prepared by conjugate addition of grignard reagents to the corresponding α,β-unsaturated esters (ethyl magnesium bromide + crotonate for **1c** and **1e**, methyl magnesium iodide + pent-2-enoate for **1d**). The diastereoselectively labeled amides **1a** and **1b** were prepared starting from *cis*- and *trans*-2-butene oxide, respectively, which were then reduced, tosylated and converted to the desired amides by using well established synthetic procedures [15b]. The final products were purified by recrystallization from chloroform/hexane and spectroscopically characterized by ^{1}H NMR and GC–MS.

3. Experimental results

The outline of the paper is as follows: after having ascertained the resemblance between the gas-phase behaviors of photoionized valeramide and 3-methyl valeramide, the different fragmentation paths of the latter are discussed with the prime focus on the McLafferty rearrangement and related processes. Kinetic modeling of the experimentally observed

[1] The very first experiments were conducted with an OQ-arrangement of CERISES, since the second quadrupole was only incorporated in the course of the study. Partial repetition of earlier experiments with the upgraded setup proved the effect of the additional quadrupole on the relative abundances to be negligible.

[2] Note that the syntheses lead to racemic mixtures of diastereomerically pure compounds (>98% de). Thus, **1a** corresponds to a 1:1 mixture of *(3R,4S)*-3-methyl-[4-D_1]-valeramide and *(3S,4R)*-3-methyl-[4-D_1]-valeramide. Likewise, **1b** is a mixture of *(3R,4R)*-3-methyl-[4-D_1]-valeramide and *(3S,4S)*-3-methyl-[4-D_1]-valeramide. For the sake of simplicity, only one of the two enantiomers is shown in the mechanistic schemes. Similarly, **1** and **1c**–**e** were studied as racemic mixtures. As we are probing only diastereomeric effects, this has no consequences for the data analysis.

labeling patterns provides insights into the competition of the various channels and finally into the diastereoselective discrimination operative in the McLafferty reaction of the title compound.

Recently, we have reported a detailed study on the fragmentation behavior of ionized valeramide [10–12]. The main channel upon photoionization of this amide corresponds to the McLafferty rearrangement, initiated by hydrogen transfer from the γ-C-atom to the carbonyl oxygen, followed by β-C–C bond cleavage. Losses of C_1- and C_2-units can compete to some extent and are both also initiated by H-rearrangements, except for a minor contribution of ethyl elimination occurring via a direct C(3)–C(4) bond cleavage at elevated energies.

Not surprisingly, the ionization energy (IE) of 3-methyl valeramide (9.36 ± 0.04 eV) is slightly lower than that of valeramide (9.40 ± 0.03 eV) [10]. The stabilizing effect of alkyl branches in organic radical cations, manifesting in lower IE values compared to the non-branched analogues, has been observed for various types of aliphatic compounds, as there are paraffins, alcohols, aldehydes, ketones, acids, esters, and amines [17].

The general fragmentation pattern of photoionized 3-methyl valeramide (**1**) resembles those of the linear congeners valeramide [10] and caproamide [9]. The dominating McLafferty rearrangement leads to the enol form of ionized acetamide ($m/z = 59$). Minor pathways correspond to losses of neutral methyl, ethyl, and propyl radicals, as well as ethene (Fig. 1). For the sake of clarity, let us group the different fragmentations into three categories, in analogy to the mechanistic pathways in the dissociative photoionization of valeramide [10]: the "McLafferty region", the "C_1 region", and the "C_2/C_3 region".

The mass spectra obtained at various photon energies ($E_{h\nu}$) provide an overview of the energy dependence of the different fragmentation routes (Fig. 2). The McLafferty rearrangement occurs close to the photoionization threshold, and rises quickly in intensity to cover more than 80% of the total

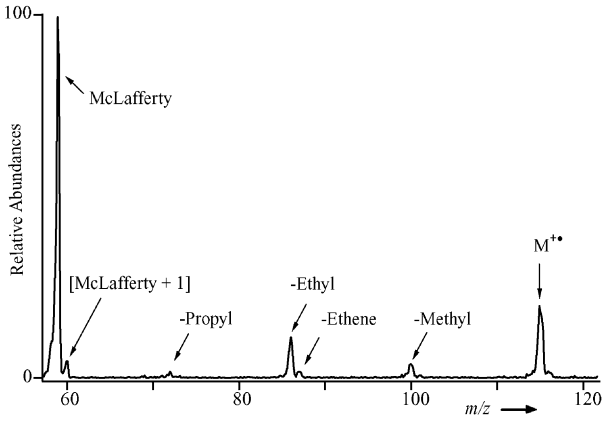

Fig. 1. Photoionization mass-spectrum of 3-methyl valeramide **1** at $E_{h\nu} = 11.5$ eV (without LiF filter). The spectrum includes contributions from ^{13}C-isotopomers and from ionization events by higher-order photons.

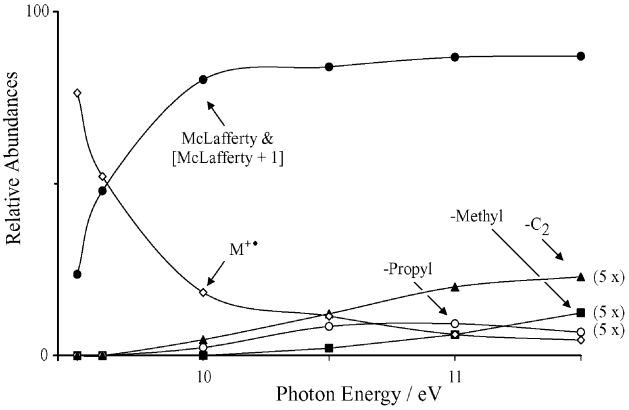

Fig. 2. Breakdown diagram of $\mathbf{1d}^{+\bullet}$. The given (^{13}C-corrected) curves show the relative abundances of the parent ion (◊) and McLafferty-related reactions (●), propyl- (○), C_2- (▲), and methyl-losses (■). The three latter curves are multiplied by a factor of 5.

ion current; the parent ion diminishes in parallel. Expulsions of $CH_3^\bullet$ and C_2/C_3-units require somewhat higher energies. Compared to the dominant McLafferty processes, these fragmentations do never attain important abundances and remain weak throughout the range of $E_{h\nu}$ studied; their discussion is therefore kept to a minimum.

3.1. The "McLafferty region"

As will be detailed in the course of this section, ionized 3-methyl valeramide $\mathbf{1}^{+\bullet}$ dissociates via four different McLafferty-related pathways, and some of the resulting product ions have the same elemental compositions or are isobaric with each others. Therefore, it is more reasonable to refer to the fragmentation products of the "McLafferty region" by their mass-to-charge ratios ($m/z = 59$–62) rather than by the masses of the expelled neutral molecules. Thus, the "McLafferty region" of **1** comprises signals at $m/z = 59$ and 60 while the labeled parent ions also yield ions at $m/z = 61$; a signal at $m/z = 62$ is conceivable as well, but was never observed in quantities significantly exceeding the expected ^{13}C-contribution of $m/z = 61$.

The major McLafferty (McL) reaction of $\mathbf{1}^{+\bullet}$ (Scheme 1) yields the enol form of ionized acetamide, $[H_2C{=}C(OH)NH_2]^{+\bullet}$, in that an initial [1,5]-H shift of a γ-hydrogen to the carbonyl oxygen ($\mathbf{1}^{+\bullet} \rightarrow \mathbf{2}^{+\bullet}$) is followed by C(2)–C(3) bond cleavage to expel butene ($\mathbf{2}^{+\bullet} \rightarrow \mathbf{3}^{+\bullet} + C_4H_8$). This process dominates the dissociation behavior of $\mathbf{1}^{+\bullet}$ and proceeds with a very low barrier ($AE(McL) = 9.52 \pm 0.02$ eV, see below). In addition, there are two competing, McLafferty-related processes, which obscure the product distribution in the "McLafferty region" of isotopomeric 3-methyl valeramides due to mass overlaps.

The first, and rather obvious complication arising from the choice of the model system is the presence of a second possibility for a [1,5]-H shift in that not only C(4), but also C(4′) serves as a potential site for the McLafferty reaction (conformers $\mathbf{1}_1{}^{+\bullet}$ and $\mathbf{1}_2{}^{+\bullet}$ in Scheme 1). The pronounced

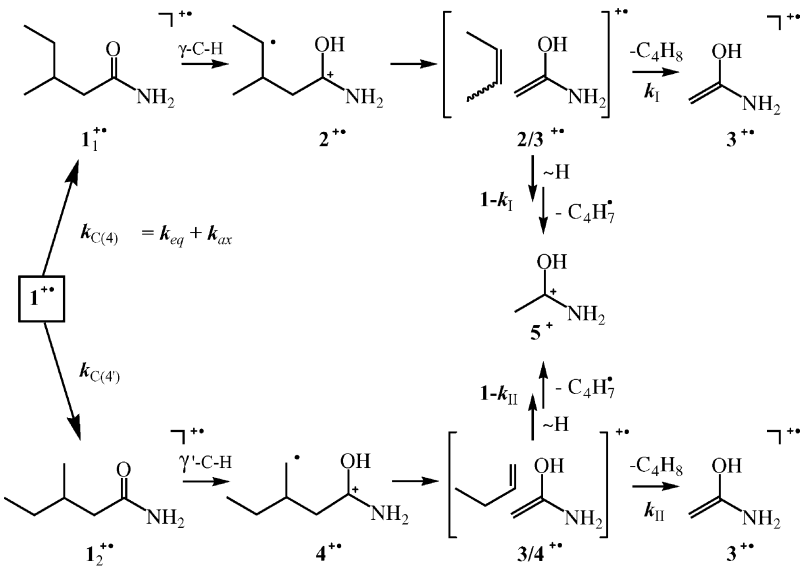

Scheme 1.

formation of ions with both $m/z = 59$ and 60 from the respectively γ- and γ′-labeled isotopomers **1c**$^{+\bullet}$ and **1d**$^{+\bullet}$ reveals that both positions compete effectively. In order to distinguish these two routes, the McLafferty reaction with the initial hydrogen transfer occurring from C(4) is referred to as McL_I and that involving the C(4′)-position as McL_{II}. Unlike ionized valeramide, for the unlabeled compound **1**$^{+\bullet}$ a notable signal at $m/z = 60$ is observed (clearly above the ^{13}C-contribution), which can be assigned to the occurrence of a second hydrogen-atom transfer following the McLafferty rearrangement. Such a McLafferty reaction with double hydrogen transfer, the so-called [McLafferty + 1] reaction [4,18], is well-known for ketones [19,20], aliphatic [21] and cyclic [4] carboxylic acids, esters [18,22,23], thioesters, phosphates, and sulfones [18]. Given that 3-methyl valeramide offers two sites for the first hydrogen transfer, C(4) and C(4′), it is to be assumed that each of them can be followed by a second hydrogen migration. Thus, there are two additional competitors to the two classical McLafferty reactions: $[McL + 1]_I$ and $[McL + 1]_{II}$ reaction (**1**$^{+\bullet}$ → **2**$^{+\bullet}$ → **5**$^{+\bullet}$ and **1**$^{+\bullet}$ → **4**$^{+\bullet}$ → **5**$^{+\bullet}$; Scheme 1).

For an investigation of the energy dependence of the McLafferty-related fragmentations, mass-spectra of the "McLafferty region" were taken for the isotopomers **1**$^{+\bullet}$–**1e**$^{+\bullet}$ at $E_{h\nu} = 9.6$, 10, and 11 eV and at improved mass resolution (Table 1). A priori we are interested in the kinetic effects of the McL_I reaction, i.e., the kinetic isotope effect (KIE_I) associated with the [1,5]-H shift from C(4) and particularly the steric effect (SE) that distinguishes the two diastereotopic hydrogens at C(4). Note that the SE not only comprises the different rate constants for the transfer of the diastereotopic H(D) atoms but also any possible difference in their associated KIEs, so that a diastereotopic differentiation of KIE_I is obsolete. A first estimation of the steric effect is achievable from the ratios of $m/z = 59$ and 60 for the diastereomers **1a**$^{+\bullet}$ and **1b**$^{+\bullet}$; the mass spectra at 11 eV (Fig. 3), for example, reveal a significant difference in the "McLafferty region" which unambiguously proves the operation of a substantial SE. For a more detailed analysis of the McL_I reaction, however, this process needs to be disentangled from the competing McL_{II} route and the [McLafferty + 1] contri-

Table 1
Ion masses (m/z in amu) and normalized intensities[a] in the "McLafferty region" observed in the PI spectra of **1** and its isotopomers at three different photon energies ($E_{h\nu}$)

$E_{h\nu}$	9.6 eV			10 eV			11 eV		
	59	60	61	59	60	61	59	60	61
1	81	19		94	6		97	3	
1a	45	46	9	57	39	4	61	37	2
1b	63	29	8	80	19	1	84	15	1
1c	31	62	7	46	51	3	51	47	2
1d	67	26	7	65	33	2	61	38	1
1e	84	13	3	95	4	0.6	97	2	0.4

[a] Normalized to $\Sigma = 100$ after ^{13}C-correction. For error bars see Appendix B. Intensities >1 given as integers; rounding errors may occur.

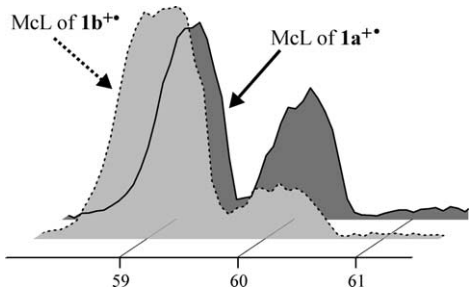

Fig. 3. "McLafferty regions" of the *anti*- and *syn*-diastereomers **1a**$^{+\bullet}$ and **1b**$^{+\bullet}$ at $E_{h\nu} = 11$ eV. The McL_I reaction proceeding via D-transfer ($m/z = 60$) is more favored in the case of the *anti*-[4-D_1]-diastereomer (**1a**$^{+\bullet}$) than in the case of the *syn*-analogue (**1b**$^{+\bullet}$), irrespective of the KIE_I which equally favors the McL_I rearrangement via H-transfer ($m/z = 59$).

butions [24]. A rough estimation of the branching ratios between the McL_I and McL_{II} channels can be derived from the $m/z = 59{:}60$ ratios of $\mathbf{1c}^{+\bullet}$ and $\mathbf{1d}^{+\bullet}$, as these isotopomers are completely labeled in the respective γ- and γ′-positions. Thus, the McL_I route largely predominates at low photon energies, whereas the McL_{II} process competes efficiently at elevated $E_{h\nu}$. Isotopomer $\mathbf{1e}^{+\bullet}$ helps to unravel the mechanism of the superimposing [McLafferty + 1] reactions (see below).

At this point it has to be stated that only a consideration of all isotopomers provides a quantitative understanding of the strongly coupled kinetic parameters. For the data at 11 eV, where the double hydrogen transfer is comparably weak, a quantitative correction for the latter appears reasonable which then allows for an approximate analysis of the McL_I and McL_{II} related parameters [25]. For a comprehensive analysis of all data, however, a complete kinetic modeling of all effects and branching ratios is inevitable. In order to guide such a model, the experimental findings are first analyzed qualitatively in order to derive some helpful orientation.

3.1.1. The steric effect

Fig. 3 proves that the two diastereomers differ considerably in the outcome of their McLafferty reactions. At all photon energies studied, $\mathbf{1b}^{+\bullet}$ shows a markedly higher $m/z = 59{:}60$ ratio than $\mathbf{1a}^{+\bullet}$ (Table 1). While in both cases, a KIE_I hinders the formation of $m/z = 60$, for $\mathbf{1b}^{+\bullet}$, a steric effect acts as an additional hindrance which obviously disfavors the production of $m/z = 60$ in favor of $m/z = 59$. For $\mathbf{1a}^{+\bullet}$, the SE works in the opposite direction and depletes the formation of $m/z = 59$. A simple and convincing rationale for the steric effect is that the initial step of the McL_I reaction, the γ-H-shift from C(4) to oxygen ($\mathbf{1}^{+\bullet} \rightarrow \mathbf{2}^{+\bullet}$) occurs via a chair-like transition structure (Scheme 2). While transfer of a γ-hydrogen in $\mathbf{1a}^{+\bullet}$ is only possible if one of the two methyl groups of the cyclic transition structure, C(4′) or C(5), adopts an energy demanding, axial position (e.g., structure **ax-1a/2a**$^{+\bullet}$), whereas deuterium migration can take place through a preferable, double-equatorial conformation (structure **eq-1a/2a**$^{+\bullet}$). In contrast, a γ-H-shift from C(4) to oxygen for $\mathbf{1b}^{+\bullet}$ is sterically preferred over γ-D-transfer. Note, however, that for both diastereomers a considerable percentage of ions at $m/z = 59$ results from McL_{II} reaction, which makes it impossible to evaluate quantitatively the magnitude or at least the ratio of KIE_I and SE from the spectra of $\mathbf{1a}^{+\bullet}$ and $\mathbf{1b}^{+\bullet}$ alone, not to mention the influence of the additional overlaps in the particular m/z region caused by the [McLafferty + 1] channels.

3.1.2. Competition of the γ- and γ′-positions

Particularly instructive with respect to the branching ratios of the competing McLafferty reactions are $m/z = 59$ and 60 for $\mathbf{1c}^{+\bullet}$ and $\mathbf{1d}^{+\bullet}$. The McL_I reaction yields $m/z = 60$ for $\mathbf{1c}^{+\bullet}$ and $m/z = 59$ for $\mathbf{1d}^{+\bullet}$, whereas the McL_{II} reaction leads to $m/z = 59$ for $\mathbf{1c}^{+\bullet}$ and $m/z = 60$ for $\mathbf{1d}^{+\bullet}$. With increasing $E_{h\nu}$, the $m/z = 59{:}60$ ratio increases for $\mathbf{1c}^{+\bullet}$ and decreases for $\mathbf{1d}^{+\bullet}$ (Table 1). Accordingly, the McL_{II} route gains in importance at the expense of McL_I as more internal energy is deposited in the parent ions formed upon photoionization. For a more quantitative analysis of the $m/z = 59{:}60$ ratios of $\mathbf{1c}^{+\bullet}$ and $\mathbf{1d}^{+\bullet}$, the composite origin of ions $m/z = 60$ has to be taken into account. The majority of $m/z = 60$ stems from McLafferty rearrangements involving a deuterium from a γ-

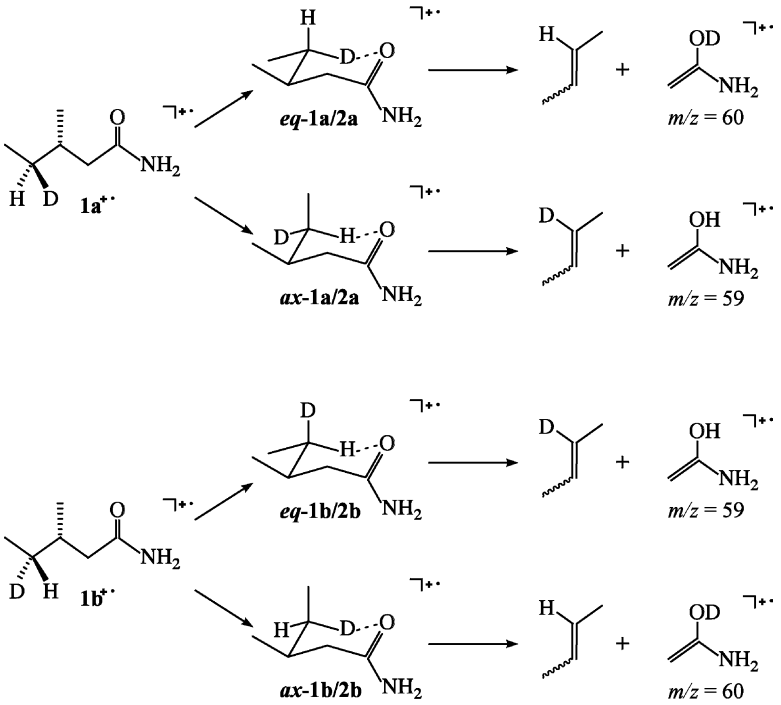

Scheme 2.

or γ′-position and is hence subject to primary and, possibly, secondary kinetic isotope effects (inverse KIEs for the [1,5]-H-shifts are excluded, see Appendix A). A minor contribution results from double H-transfer in the course of the [McLafferty + 1] reactions. The KIEs cause a decrease of the intensities of $m/z = 60$ (which is much more pronounced than the gain by the additional contributions from [McLafferty + 1] processes), so that at all energies the $m/z = 59{:}60$ ratio of $\mathbf{1d}^{+\bullet}$ is somewhat larger than the reciprocal ratio $m/z = 60{:}59$ of $\mathbf{1c}^{+\bullet}$. The effective branching ratios of McL_I and McL_{II} can be expected to be in between the reciprocal intensity ratios of $\mathbf{1c}^{+\bullet}$ and $\mathbf{1d}^{+\bullet}$ that is 2.0–2.6 at 9.6 eV, 1.1–2.0 at 10 eV, and 0.9–1.9 at 11 eV. The prevalence of the McL_I reaction over McL_{II}, despite the numerical inferiority of the C(4)–H bonds vis-à-vis the C(4′)–H bonds, is in perfect agreement with the notion of a primary C–H bond being more difficult to cleave than a secondary C–H bond [26]. As the differences in bond strengths matter less with increasing $E_{h\nu}$, both pathways compete effectively at 11 eV.

The two McLafferty routes are restricted by the initial C–C bond rotations required to access suitable conformers for the initial [1,5]-H-transfers from C(4) or C(4′) to the carbonyl oxygen. In the case of unbranched valeramide, the conformational barrier constitutes in fact the bottle-neck of the (at room temperature) kinetically controlled path, while the [1,5]-H migration is only a rate-contributing step [11]. Assuming a similar scenario for the McLafferty reactions of $\mathbf{1}^{+\bullet}$, the branching between the C(4)- and the C(4′)-routes can be regarded as being quasi-irreversible. Thus, any ions that passed the conformational barrier in the C(4)-route are bound to dissociate via McL_I or $[McL + 1]_I$.

3.1.3. The [McLafferty + 1] rearrangement

The mass spectra of the unlabeled compound $\mathbf{1}^{+\bullet}$ at various photon energies provide a direct measure for the ratio of the McLafferty and [McLafferty + 1] reactions as a function of $E_{h\nu}$. Double hydrogen transfer is of considerable intensity close to threshold (i.e., 19% at 9.6 eV), but decreases rapidly with higher energies (6% at 10 eV and 3% at 11 eV). Obviously, the [McLafferty + 1] reaction is not constrained by high barriers, so that it takes place already with very little excess energy ($AE([McL + 1]) = 9.43 \pm 0.04$ eV versus $IE(\mathbf{1}^{+\bullet}) = 9.36 \pm 0.04$ eV). On the other hand, a sequence of consecutive H-migrations requires rather extensive rearrangement. At this stage, we invoke the concept of ion-neutral complexes, for which many examples in the chemistry of organic radical cations can be given [27,28], and which has been proven extremely compelling for the interpretation of competing McLafferty-related reactions [29,30]. Apparently, the lifetimes of the intermediary ion-neutral complexes $\mathbf{2}/\mathbf{3}^{+\bullet}$ and $\mathbf{3}/\mathbf{4}^{+\bullet}$ (Scheme 1) are crucial for the occurrence of a second H-shift, which explains why the [McLafferty + 1] signals rapidly lose intensity with increasing photon energies and hence decreasing number of parent ions with low internal energy content. In contrast, single H-transfer can still take place at shorter ion lifetimes, resulting in a pronounced difference in slope for the appearance energy curves of the McLafferty and the [McLafferty + 1] product ions (Fig. 4).

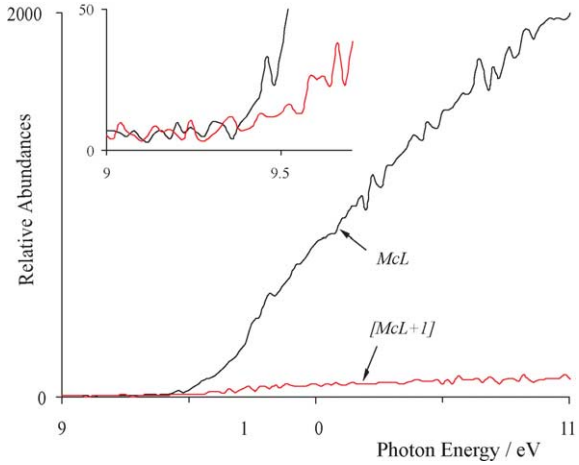

Fig. 4. Appearance energy curves of the McLafferty (black) and [McLafferty + 1] (red) product-ions of photoionized **1e** (i.e., $m/z = 59$ vs. $m/z = 60$ and 61).

Deuteration at C(5) in isotopomer $\mathbf{1e}^{+\bullet}$ allows for some inference about the mechanism of the [McLafferty + 1] rearrangement. Obviously, part of the [McLafferty + 1] ions produced contains a hydrogen atom (or rather deuterium in the case of $\mathbf{1e}^{+\bullet}$) from the C(5) position ($m/z = 61$), but the importance of [McLafferty + 1] reactions not involving this position (giving ions with $m/z = 60$) is clearly superior[3] at any energy $E_{h\nu}$.

Whereas several mechanisms of the [McLafferty + 1] rearrangements are conceivable, only those are realistic which agree with the notions of low barriers and sufficiently long lifetimes of the intermediary ion-neutral complexes. A quite appealing route in this respect is a preferred transfer of the second hydrogen atom from an allylic position of the butene fragment in the ion-neutral complexes $\mathbf{2}/\mathbf{3}^{+\bullet}$ and $\mathbf{3}/\mathbf{4}^{+\bullet}$ (Scheme 1), so that the eventually eliminated neutral $C_4H_7^{\bullet}$ as well as the associated transition structure can profit from allylic stabilization. The assumed long lifetimes may as well allow partial equilibration of the "butene hydrogens" in $\mathbf{2}/\mathbf{3}^{+\bullet}$ or $\mathbf{3}/\mathbf{4}^{+\bullet}$. Results obtained for the interaction of propene with the enol of ionized acetic acid disproved the reversibility of the hydrogen-transfer from the alkene to the enol's methylene group; yet, a rapid, reversible exchange between the alkene hydrogens and the hydroxyl hydrogens was observed [31]. Furthermore, experiments by Weber et al. [32] suggest a considerable participation of all "propene-hydrogens" in the [McLafferty + 1] reaction of ionized pentanoic acid, although complete loss of positional identity was not observed and the participation of allylic hydrogens was clearly favored. The butene hydrogens in 3-methyl valeramide (**1**) may accordingly equilibrate in those ion-neutral complexes

[3] The (non-rounded) intensities for $\mathbf{1e}^{+\bullet}$ yield ratios $m/z = 60{:}m/z = 61$ of 5.0 (9.6 eV), 7.7 (10 eV) and 5.3 (11 eV).

which possess sufficiently long lifetimes to fragment via the [McLafferty + 1] path. That is, the first hydrogen shift may partially be reversible [30] and thus allow for some H/D-equilibration when **2**/**3**$^{+\bullet}$ and **3**/**4**$^{+\bullet}$ are sufficiently long-lived. However, a fully statistical participation of the butene's hydrogen/deuterium atoms is ruled out by the absence of $m/z = 62$ from **1c**$^{+\bullet}$ and **1d**$^{+\bullet}$, whereas a partial H/D-exchange below the experimental detection limit cannot be discarded.

As four McLafferty-related reactions, McL_I and McL_{II}, $[McL + 1]_I$ and $[McL + 1]_{II}$, compete with each other, any labeling will affect the branching ratios due to the operation of kinetic isotope effects. Especially channels of low intensity (like the [McLafferty + 1] reactions) are bound to suffer from the operation of isotopically sensitive branching, which means that even small intrinsic KIEs may give rise to large variations in the observed product distributions. Depending on the size of the intrinsic KIEs, this may lead to extremely large (or small) apparent KIEs [33].

3.1.4. Appearance energies of the McLafferty and [McLafferty + 1] product ions

The appearance curves of the McLafferty and the [McLafferty + 1] rearrangements do not show a linear rise, but display some low-energy tailing (width ∼0.1 eV) attributed to thermal contributions. Thus, some of the McLafferty product ions are already formed close to the onset of photoionization: for example, the [McLafferty + 1] channel is even visible directly at the ionization onset, McL_I occurs just 0.04 eV, and McL_{II} commences 0.10 eV above the photoionization threshold. Note that the low demand in excess energy (0.04 eV) compares well with the respective demand of the unbranched system (0.03 eV excess energy). The AEs discussed in the following are obtained by linear extrapolation of the curves without consideration of thermal contributions and therefore result in slightly higher values.

The AEs of particularly instructive signals in the "McLafferty regions" of selected isotopomers are given in Table 2. For the McL_I reaction, single-ion monitoring of $m/z = 59$ from **1d**$^{+\bullet}$ yields $AE(McL_I) = 9.52 \pm 0.02$ eV, that is the McLafferty reaction commences 0.16 eV above the photoionization threshold of the molecule. The analogous reaction involving a primary C(4′)–H bond needs slightly more energy: $AE(McL_{II}) = 9.58 \pm 0.03$ eV for $m/z = 59$ from **1c**$^{+\bullet}$. The possible operations of primary and secondary KIEs do not affect the AEs to considerable extents, as the onsets for the formations of ions with $m/z = 60$ from **1c**$^{+\bullet}$ (9.52 ± 0.02 eV) and **1d**$^{+\bullet}$ (9.57 ± 0.02 eV) fully confirm the AEs of McL_I and McL_{II}, respectively, suggesting that those KIEs are at best modest. As expected, the appearance energies of $m/z = 59$ from **1**$^{+\bullet}$, **1b**$^{+\bullet}$, and **1e**$^{+\bullet}$ are in between those of McL_I and McL_{II}. Finally, single-ion monitoring of $m/z = 60$ from **1e**$^{+\bullet}$ leads to $AE([McL + 1]) = 9.43 \pm 0.04$ eV, substantiated by the upper limit of 9.47 ± 0.07 eV given by the (probably KIE-affected) appearance curve of the respective deuterated ions with $m/z = 61$.

Table 2
Appearance energies (in eV) of particularly instructive fragment ions (m/z in amu) in the "McLafferty region" of selected isotopomers of 3-methyl valeramide

m/z	59	60	61
1	9.56 ± 0.04		
1b	9.52 ± 0.02	9.43 ± 0.03	
1c	9.58 ± 0.03	9.52 ± 0.02	
1d	9.52 ± 0.02	9.57 ± 0.02	
1e	9.56 ± 0.04	9.43 ± 0.04	9.47 ± 0.07

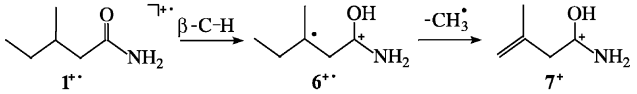

Scheme 3.

3.2. Minor fragmentation channels: losses of C_1-, C_2-, and C_3-units

The minor fragmentations of the methyl and C_2/C_3 regions are comprised for the sake of completeness. However, as mentioned above, given their close similarity to the corresponding fragmentations of ionized valeramide [10] as well as their low abundances, only a qualitative analysis is presented.

3.2.1. The "C_1 region"

Isotopomers **1**$^{+\bullet}$–**1d**$^{+\bullet}$ form exclusively $[M - 15]^+$ fragments, whereas C(5)-deuterated **1e**$^{+\bullet}$ yields a signal at $[M - 18]^+$; thus, a specific loss of the terminal C(5)-methyl group takes place. This dissociation pathway shows the same regiochemistry and energy demands as for ionized valeramide [10,11], and the corresponding mechanism is therefore adopted accordingly (Scheme 3): β-H-transfer to the carbonyl oxygen (**1**$^{+\bullet} \rightarrow$ **6**$^{+\bullet}$) is followed by C(4)–C(5) bond scission (**6**$^{+\bullet} \rightarrow$ **7**$^{+}$). Single-ion monitoring yields an appearance curve with a very smooth slope prior to a steeper rise. Thus, the first signal distinguishable from the noise level appears already at $AE(-CH_3) = 10.05 \pm 0.07$ eV (from **1**$^{+\bullet}$), but noteworthy abundances are only reached at much higher energies (second onset at 10.68 ± 0.07 eV). The slightly higher value derived from **1e**$^{+\bullet}$, $AE(-CD_3) = 10.12 \pm 0.04$ eV, may indicate the operation of a modest secondary KIE, which would agree with the theoretical finding for the demethylation of ionized valeramide [11] that the C–C bond cleavage represents the highest barrier of this kinetically controlled path. The considerable energy demand for the first appearance of methyl loss (0.69 eV excess energy with respect to IE(1)) agrees well with the barrier height predicted by theory for the rate determining C–C bond rupture in valeramide (0.63 eV excess energy at 298 K). However, the experimental value derived for valeramide was even higher (about 1.5 eV excess energy[4]),

[4] In Ref. [10], the reported upper limit of the appearance energy was deduced from a series of mass spectra recorded at various photon energies.

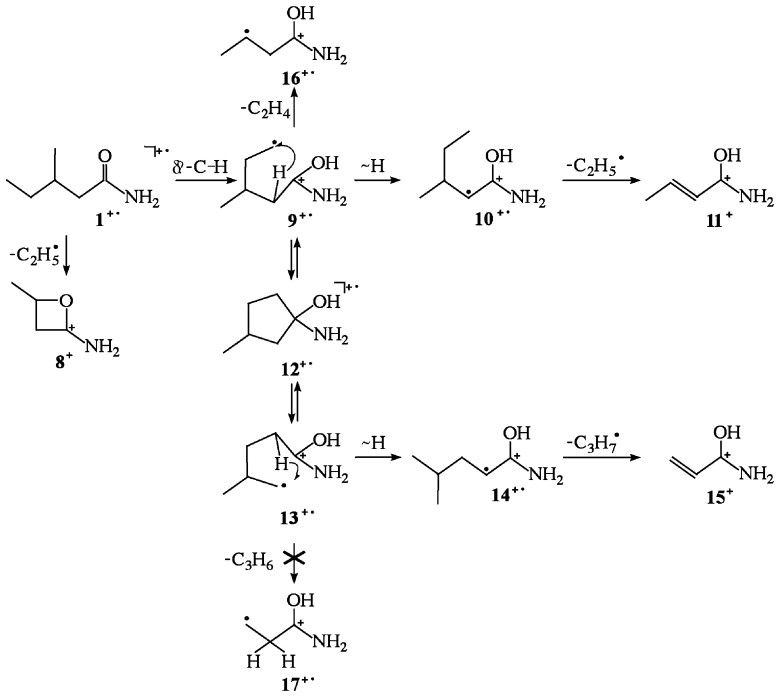

Scheme 4.

which has been attributed to a substantial competitive kinetic shift caused by the competing major channels. For 3-methyl valeramide, the methyl loss is also more energy demanding than the dominating McLafferty related processes, and is hence likely to be subject to a competitive shift as well. In fact, the second onsets (10.68 ± 0.07 eV for $[\mathbf{1} - 15]^{+\bullet}$ and 10.62 ± 0.06 eV for $[\mathbf{1e} - 18]^{+\bullet}$, corresponding to 1.32 and 1.26 eV excess energy) compare reasonably well with the mentioned experimental findings for the valeramide system (about 1.5 eV excess energy, see footnote 4).

3.2.2. The "C_2/C_3 region"

Assuming that the additional methyl group in **1**, compared to valeramide, does not drastically change the overall fragmentation behavior of the radical cation, the previously derived fragmentation scheme developed for ionized valeramide is also applied to $\mathbf{1}^{+\bullet}$ with some minor adjustments to account for the structural modification in the backbone. Thus, the mechanisms depicted in Scheme 4 indeed agree well with the observed product distributions in the C_2/C_3 region for all isotopomers. For example, δ-H transfer to the carbonyl oxygen leads to the δ-distonic radical cation $\mathbf{9}^{+\bullet}$, from which several dissociation paths are possible. An indirect ethyl loss preceded by a [1,4]-H shift and subsequent C(3)–C(4) bond scission ($\mathbf{9}^{+\bullet} \rightarrow \mathbf{10}^{+\bullet} \rightarrow \mathbf{11}^{+}$) is quite facile ($[\mathbf{1e} - 31]^{+}$ gives $AE(-C_2H_5{}^{indir}) = 9.56 \pm 0.08$ eV), and its energy demand compares well with that of the respective indirect ethyl expulsion from ionized valeramide (0.20 eV excess energy for 3-methyl valeramide versus 0.18 eV for valeramide). In competition with the indirect ethyl loss, a propyl elimination takes place. This route is accessible by skeletal rearrangement $\mathbf{9}^{+\bullet} \rightleftharpoons \mathbf{12}^{+\bullet} \rightleftharpoons \mathbf{13}^{+\bullet}$, which brings about an equilibration between the δ-distonic ions $\mathbf{9}^{+\bullet}$ and $\mathbf{13}^{+\bullet}$. The propyl loss is of low abundance and has a notably higher energy demand ($[\mathbf{1e} - 44]^{+\bullet}$ gives $AE(-C_3H_7{}^{indir}) = 9.90 \pm 0.12$ eV) than the indirect ethyl loss. The heats of formation of the products of these two equilibrated channels ($\mathbf{11}^{+} + C_2H_5^{\bullet}$ versus $\mathbf{15}^{+} + C_3H_7^{\bullet}$) differ by about 0.30 eV,[5] which can be ascribed to the stronger stabilizing effect of methylation of a double bond (for the exit channel $\mathbf{11}^{+} + C_2H_5^{\bullet}$) compared to methylation of an alkyl radical (for the exit channel $\mathbf{15}^{+} + C_3H_7^{\bullet}$). The AE difference of 0.34 eV between the indirect ethyl and propyl eliminations is thus readily explained by the different energetics of the exit channels and is accordingly ascribed to thermodynamic control.

The intermediate $\mathbf{9}^{+\bullet}$ can also expel ethene upon immediate C(3)–C(4) bond rupture ($\mathbf{9}^{+\bullet} \rightarrow \mathbf{16}^{+\bullet}$); an analogous route from $\mathbf{13}^{+\bullet}$, leading to an expulsion of propene, is not observed ($\mathbf{13}^{+\bullet} \not\rightarrow \mathbf{17}^{+\bullet}$). Single-ion monitoring of $[\mathbf{1e} - 30]^{+\bullet}$ yields $AE(-C_2H_2D_2)$ of about 9.55 eV. The markedly lower energy demand in comparison to the corresponding ethene loss from ionized valeramide (0.19 eV excess energy for 3-methyl valeramide versus 0.6 eV for valeramide) can be attributed to the stabilizing effect of the additional methyl group in the transition structure of the C–C bond cleavage, $\mathbf{9}^{+\bullet} \rightarrow \mathbf{16}^{+\bullet}$.

[5] The energetic differences are based on relative energies at 0 K calculated at the B3LYP/6-311++G**//B3LYP/6-31G* level of theory, where the ZPEs, calculated with B3LYP/6-31G*, were used in the conversion to relative energies at 0 K according to B3LYP calculations.

The fact that C(5)-deuterated $\mathbf{1e}^{+\bullet}$ not only yields ions $[M-31]^+$ according to the indirect ethyl loss ($\mathbf{1}^{+\bullet} \rightarrow \mathbf{9}^{+\bullet} \rightarrow \mathbf{10}^{+\bullet} \rightarrow \mathbf{11}^{+}$), but also exhibits a signal at $[M-32]^+$, indicates the occurrence of additional, direct ethyl elimination from the terminus[6] as already observed for valeramide. Thus, direct C(3)–C(4) bond cleavage ($\mathbf{1}^{+\bullet} \rightarrow \mathbf{8}^{+}$) first becomes noticeable at $AE(-C_2H_5{}^{dir}) = 9.94 \pm 0.07$ eV (for $[\mathbf{1e}-32]^+$), which corresponds to an excess energy of 0.58 eV. Similar to the methyl loss, the appearance curve of $[\mathbf{1e}-32]^+$ has an ill-defined slope. Linear extrapolation of the latter, steeper part of the rise gives 10.55 ± 0.05 eV, which is again attributed to a competitive kinetic shift caused by the dominating McLafferty-related processes and the low-energy channels of the C_2/C_3-region (i.e., indirect ethyl loss and ethene elimination). The derived value of 1.19 eV excess energy compares well with about 1.1 eV (see footnote 4) reported for valeramide.

4. Kinetic modeling of the "McLafferty region"

Our key interest concerns diastereoselective discrimination in McLafferty rearrangements for which 3-methyl valeramide is used as a model system. As demonstrated, the introduction of a methyl group at C(3) does not largely change the general fragmentation pattern compared to the parent compound valeramide. However, occurrence of the [McLafferty + 1] process and more seriously the function of the newly introduced methyl group as an additional site for a [1,5]-H transfer hinder a straightforward quantitative analysis of the measured fragment-ion abundances with respect to the steric effect (SE). While the operation of SE is quite obvious from a mere comparison of the spectra of diastereomers $\mathbf{1a}^{+\bullet}$ and $\mathbf{1b}^{+\bullet}$ (Fig. 3), a quantitative determination of the SE needs to acknowledge the various competitive channels. To this end, we pursue the concept of a comprehensive kinetic modeling which has been applied successfully in several systems of rather different types [10,34–36].

4.1. Modeling of the experimental data

Modeling of the relative abundances in the "McLafferty region" was carried out using two alternative sets of kinetic equations which differ only in the description of the [McLafferty + 1] process (Appendix A). The first set describes the system under assumption of an allylic mechanism for the second hydrogen transfer. In addition, the extreme case of a fully statistical participation of the "butene hydrogen/deuterium atoms" in the second H-shift is modeled to judge quantitatively the effects of possible H/D-equilibration (for further modeling details, see Appendix C). Both models use the same parameters. The branching of the first H-transfer is described by the normalized rate constants k_{eq}, k_{ax}, and $k_{C(4')}$ with $k_{eq} + k_{ax} + k_{C(4')} = 1$ (Scheme 1). Here, k_{eq} describes the H-migration from C(4) which can occur via a double equatorial transition structure (**eq-1**/$\mathbf{2}^{+\bullet}$, Scheme 2), k_{ax} stands for the H-shift from C(4) which would force one methyl group in an axial alignment (**ax-1**/$\mathbf{2}^{+\bullet}$), and $k_{C(4')}$ represents H-migration from C(4′). The competition between C(4) and C(4′) reactivity is thus expressed by ($k_{eq} + k_{ax}$) versus $k_{C(4')}$; for the sake of simplicity, the sum ($k_{eq} + k_{ax}$) will be referred to as $k_{C(4)}$. Each of these routes split into two others after formation of the respective ion-neutral complexes. Thus, the C(4)-path branches to the McL_I and the $[McL + 1]_I$ reactions in a ratio k_I to $(1 - k_I)$ (see Scheme 1). Likewise, the branching of the C(4′) pathway into McL_{II} and $[McL + 1]_{II}$ is described by the ratio of k_{II} to $(1 - k_{II})$. The steric effect SE for the initial [1,5]-H transfer from C(4) ($\mathbf{1}^{+\bullet} \rightarrow \mathbf{2}^{+\bullet}$, Scheme 1) is defined as the ratio k_{eq}/k_{ax}, and the kinetic isotope effect associated with this step is referred to as KIE_I. Similar to the case of ionized valeramide [10], it is necessary to invoke a secondary kinetic isotope effect of $KIE_{sec} = 1.07$ if the γ-positions are deuterated (Appendix A). For the evaluation of the KIEs associated with C(4′)–H bond activation in step $\mathbf{1}^{+\bullet} \rightarrow \mathbf{4}^{+\bullet}$, only the isotopomer $\mathbf{1d}^{+\bullet}$ can be consulted. Therefore, one can merely derive a global value KIE_{II}* for D-transfer from C(4′). Most certainly the two remaining deuterium atoms on C(4′) both cause an additional hampering effect similar to KIE_{sec}. For the sake of better comparability with the primary KIE_I of C(4), the primary effect of C(4′) is therefore approached by a deconvolution as $KIE_{II} = KIE_{II}{}^*/KIE_{sec}^2$. For both competing [1,5]-H transfers, inverse (primary and secondary) KIEs were excluded by a preceding analysis of the experimental abundances (Appendix A). Last but not least, only a single KIE_{+1} was used to describe the (primary) kinetic isotope effects of the second hydrogen transfers in the $[McL + 1]_I$ and $[McL + 1]_{II}$ pathways. This is a reasonable simplification of the model system, in that the mechanisms and kinetic behavior of the [McLafferty + 1] rearrangements are quite similar and possible minor deviations will hardly affect the modeling, given the low intensities of these channels. As will be seen below, KIE_{+1} is indeed extremely insensitive, so there is no reason for a distinction between the different [McLafferty + 1] routes.

The allylic model leads to a satisfactory and consistent description of the system (Table 3). The hypothetical, extreme model of complete H/D-equilibration prior to the second hydrogen transfer describes the experimental data equally well (Appendix C), but, as stated above, disqualifies itself by the absence of detectable amounts of $m/z = 62$ (two-fold deuterium transfer) from $\mathbf{1c}^{+\bullet}$ and $\mathbf{1d}^{+\bullet}$. However, occurrence of partial H/D-equilibration is possible and appraised by the extreme-case modeling. At high $E_{h\nu}$ (10 and 11 eV), the resulting parameter set of the statistical model is essentially identical to the allylic one within the error margins. Only at 9.6 eV, where the [McLafferty + 1] reaction is of considerable

[6] The terminal ethyl group may not, or at least not exclusively, be expelled via the proposed direct mechanism $\mathbf{1}^{+\bullet} \rightarrow \mathbf{8}^{+}$. An alternative of initial β-H-shift from C(3) to the carbonyl oxygen, followed by 1,2-H-shift and final C(3)–C(4) bond breaking within the α-distonic intermediate is conceivable as well. For related skeletal isomerizations, see Ref. [3b].

Table 3
Normalized branching ratios and kinetic parameters obtained[a] for $E_{h\nu}$ = 9.6, 10, and 11 eV by modeling the "McLafferty region" according to the allylic and the statistical model for the second hydrogen shift

$E_{h\nu}$	9.6 eV		10 eV		11 eV	
	σ (allylic)	σ (statistical)	σ (allylic)	σ (statistical)	σ (allylic)	σ (statistical)
$k_{C(4')}$	0.38 ± 0.05	0.34 ± 0.09	0.45 ± 0.05	0.45 ± 0.05	0.48 ± 0.05	0.48 ± 0.06
k_I	0.94 ± 0.03	0.83 ± 0.02	0.93 ± 0.02	0.92 ± 0.01	0.96 ± 0.02	0.96 ± 0.01
k_{II}	0.70 ± 0.04	0.81 ± 0.08	0.95 ± 0.03	0.95 ± 0.04	0.98 ± 0.01	0.98 ± 0.02
SE	1.8 ± 0.4	1.8 ± 0.2	2.6 ± 0.2	2.7 ± 0.3	2.8 ± 0.3	2.8 ± 0.3
KIE_I	1.0 ± 0.1	1.0 ± 0.3	1.0 ± 0.2	1.0 ± 0.2	1.1 ± 0.2	1.1 ± 0.2
KIE_{II}	1.3 ± 0.4	1.7 ± 1.3	1.5 ± 0.2	1.6 ± 0.3	1.4 ± 0.3	1.4 ± 0.3
KIE_{II}*	1.5 ± 0.4	1.9 ± 1.5	1.8 ± 0.3	1.9 ± 0.4	1.6 ± 0.3	1.6 ± 0.3
KIE_{+1}[b]	2.1 ± 0.9	7.2 ± 11.5	7.1 ± 5.7	7.9 ± 7.6	4.8 ± 3.7	5.2 ± 5.0
KIE_{+1}[c]	3 ± 2	3 ± 2	3 ± 2	4 ± 2	2 ± 2	3 ± 2

[a] The values are obtained by averaging all solutions of the respective solution space, the given errors σ correspond to the respective maximal deviations.
[b] KIE_{+1} did not converge.
[c] KIE_{+1} derived from the PI mass-spectra of **1** and **1e**, see Appendix C.

intensity (19% for $\mathbf{1}^{+\bullet}$), does the statistical model result in moderately different branching ratios for the second hydrogen migrations (cf. Section 4.2). The fact that the two models display no considerable deviations in their parameter sets shows that a possible partial H/D-equilibration hardly affects the system. In the following, the kinetic parameters resulting from the allylic modeling are discussed. References to the theoretical case of a statistical participation of the butene hydrogens are only given for those parameters at 9.6 eV for which notable differences emerge.

4.2. Branching ratios

At low $E_{h\nu}$ and thus low internal energy of the ions, the [1,5]-H shift to the carbonyl oxygen preferably involves the secondary C–H bonds at C(4). However, activation of a primary C(4′)–H bond becomes more competitive at increased energies. Thus, the relative rate constant $k_{C(4')}$ increases from 0.38 at 9.6 eV to 0.45 and 0.48 at 10 and 11 eV, respectively (Table 3). The finding that an increase of internal energy enhances the propensity for cleavage of the comparably strong primary C–H bonds at C(4′) suggests some entropic preference for the activation of this particular position. With regard to the parent system of ionized valeramide, where the McLafferty rearrangement proceeds quasi-barrierless and is primarily determined by conformational constraints [10,11], a likely explanation for the energy behavior of $k_{C(4')}$ is the better accessibility of the C(4′) position, together with the larger number of C(4′)–H bonds, relative to C(4)–H.

The amount of double hydrogen transfer compared to the less complicated single hydrogen transfer is, as expected, small and reaches considerable intensity only close to threshold. As stated above, the divergence of the hypothetical statistical model from the allylic one is only considerable for the double hydrogen transfer at low $E_{h\nu}$. The allylic model requires at 9.6 eV a markedly higher percentage of $[McL + 1]_{II}$ involving the C(4′) position ($1 - k_{II} = 0.30$) than for C(4)-activation ($1 - k_I = 0.06$). This can be explained by a higher propensity of the allylic hydrogen atoms originating from the secondary carbon in $\mathbf{3}/\mathbf{4}^{+\bullet}$ to undergo a H-shift, compared to the allylic hydrogens from the primary carbons in $\mathbf{2}/\mathbf{3}^{+\bullet}$, and by the larger energy gain from a second hydrogen shift for the less stable, terminal olefin unit in $\mathbf{3}/\mathbf{4}^{+\bullet}$ compared to the internal double bond in $\mathbf{2}/\mathbf{3}^{+\bullet}$. Assuming a complete H/D-equilibration (statistical picture), the ratio between the [McLafferty + 1] and the McLafferty rearrangement is ca. 1:4 ($[1 - k_I]/k_I = 0.17/0.83$, $[1 - k_{II}]/k_{II} = 0.19/0.81$), independent of the reaction site of the first H-shift. As $E_{h\nu}$ increases and the amount of ions with low internal energies and hence sufficiently long lifetimes diminishes drastically, the ratio of direct dissociation to second hydrogen transfer from the ion-neutral complexes increases, and the difference between $(1 - k_I)$ and $(1 - k_{II})$ according to the allylic mechanism vanishes, so that the allylic and statistical model coincide.

For an overall comparison of the reaction channels, it is appropriate to compare the combined rate constants (Fig. 5a). Here, the McLafferty reactions are described by $McL_I = k_{C(4)} \times k_I$ and $McL_{II} = k_{C(4')} \times k_{II}$, the [McLafferty + 1] rearrangements by $[McL + 1]_I = k_{C(4)} \times (1 - k_I)$ and $[McL + 1]_{II} = k_{C(4')} \times (1 - k_{II})$. Thus, at 9.6 eV, 58% of the fragment ions arise from the McL_I reaction, while only half of that (27%) comes from the McL_{II} route, whose AE lies slightly above the one of McL_I (0.06 eV, see Section 3.1.4). The remaining ions are distributed to [McLafferty + 1] processes, which have low AEs but are restricted by their need for sufficient ion lifetimes to accomplish an additional H-migration. As the ionization with 9.6 eV-photons occurs close to threshold, the low internal energies allow the ion-neutral complexes $\mathbf{2}/\mathbf{3}^{+\bullet}$ and $\mathbf{3}/\mathbf{4}^{+\bullet}$ to be considerably long-lived. The $[McL + 1]_{II}$ reaction comprises the substantial amount of 11% of the total McLafferty-related processes, which is remarkable given the low amount of C(4′)-activation in general. At elevated photon energies, the [McLafferty + 1] processes decrease to values below 5% due to the shorter ion lifetimes of the majority of the parent ions.

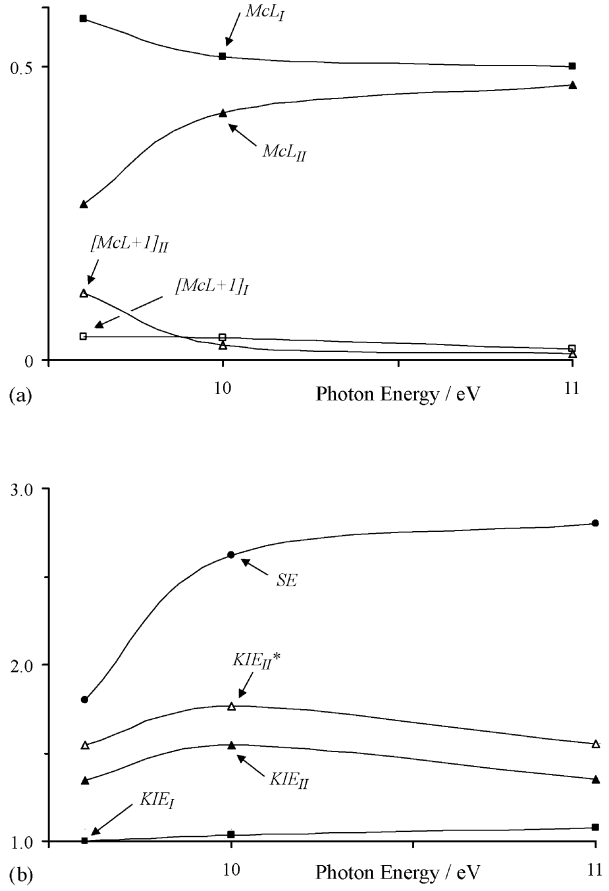

Fig. 5. Modeling results for the McLafferty-related reactions of photoionized 3-methyl valeramide **1** at $E_{h\nu}$ = 9.6, 10, and 11 eV (see text for details). (a) Combined branching ratios: McL_I (■), McL_{II} (▲), $[McL + 1]_I$ (□), and $[McL + 1]_{II}$ (△). (b) Kinetic effects: SE (●), KIE_I (■), KIE_{II}* (△), and KIE_{II} (▲).

4.3. Kinetic isotope effects

The McL_I reaction is associated with a very moderate, $E_{h\nu}$-independent KIE_I of 1.04 (Fig. 5b), which agrees nicely with the corresponding KIE of 1.03 derived for valeramide [10]. The modeling predicts the KIEs associated with [1,5]-H migration in the McL_{II} route, KIE_{II}*, to exceed those of McL_I ($KIE_I \times KIEs_{ec}$), which is consistent with the fact that the activation of a primary C–H bond at C(4′) is more energy-demanding than activation of a secondary C(4)–H bond. Deconvolution of KIE_{II}* yields a "pseudo-primary" KIE_{II} of about 1.4, also independent of $E_{h\nu}$. The higher primary KIE for the [1,5]-H migration of McL_{II} in comparison to McL_I is in agreement with the higher energy demand of the former route, which – due to the very competition of both channels – results in a more pronounced apparent KIE compared to the intrinsic one.

The low intensity of the [McLafferty + 1] channel renders the determination of the associated kinetic isotope effect less accurate. As a consequence, KIE_{+1} is rather insensitive and can adopt many values within a broad range without disturbing the system notably. However, a reasonable estimate of $KIE_{+1} = 3 \pm 2$ can be extracted from the relative abundances of the two isotopomers with the "purest" [McLafferty + 1] peaks, $\mathbf{1}^{+\bullet}$ and $\mathbf{1e}^{+\bullet}$ (Appendix C). The sole magnitude of the associated error prevents a consideration of the possible energy dependence.

4.4. Energy dependence of the steric effect

Having disentangled the various McLafferty-related processes and analyzed their respective kinetic parameters at all photon energies studied, the title question about the diastereoselectivity of the McLafferty reaction, can now be addressed in a quantitative manner. The modeling leads to SE = 1.8, 2.6, and 2.8 at $E_{h\nu}$ = 9.6, 10, and 11 eV, respectively. Interestingly, the steric effect of the C(4)-activation appears to decrease with decreasing $E_{h\nu}$ and thus with the internal energy of the parent ions (Fig. 5b). This is a rather unexpected behavior for a kinetic effect, but it can be understood within the concept of ion-neutral complexes. Already for the occurrence of the [McLafferty + 1] rearrangement, the importance of the lifetime of the ion-neutral complexes $\mathbf{2}/\mathbf{3}^{+\bullet}$ and $\mathbf{3}/\mathbf{4}^{+\bullet}$ (Scheme 1) was shown. If complex $\mathbf{2}/\mathbf{3}^{+\bullet}$ is long-lived at low energies, one could not only imagine a considerable propensity for a second hydrogen transfer competing with dissociation, but also for the reverse reaction. A retro-[1,5]-H shift from oxygen to the C(4)-atom is still in agreement with an uncoupling of C(4) and C(4′) activation, because if the conformational barriers are indeed the highest point on the potential-energy surface the reverse reaction will stop at this point. Even an only partial reversibility between $\mathbf{2}/\mathbf{3}^{+\bullet}$ and the C(4)-orientated conformer of $\mathbf{1}_1{}^{+\bullet}$ would lead to a certain epimerization of the C(4)-position and hence to a loss of steric information. At higher internal energies, the lifetime of the ion-neutral complexes is shorter with the consequence of an undiminished SE.

In a more general context, it might first appear somewhat surprising that the hydrogen transfer in the McLafferty reaction of ionized carboxamides occurs quasi-barrierless and with a negligible primary KIE on the one hand, but exhibits a pronounced SE on the other. However, it is the very nature of the quasi-barrierless reaction, which leads to the negligible KIE while the SE remains significant [8]. Thus, the question which of the two diastereotopic hydrogen atoms at C(4) is transferred to the carbonyl group is determined by the accessibility of appropriate conformations the amide radical cation needs to adopt prior to the actual hydrogen migration. These conformational changes are, however, crucially affected by the nature of the stereogenic center in 3-methyl valeramide.

5. Conclusions

The McLafferty reaction of ionized amides is associated with rather low kinetic isotope effects for the initiating hydrogen-transfer step, which can be attributed to the

fact that intramolecular hydrogen migrations in these systems occur quasi-barrierless once an appropriate conformation of the ionized functional group and the alkyl backbone is achieved. Notwithstanding, the present photoionization experiments with diastereospecifically deuterated 3-methyl valeramide analogues reveal a pronounced diastereoselective discrimination of the H-atoms in the C(4) position of the substrate. In fact, the observed steric effects of 1.8–2.8 at three different photon energies are rather large for a monofunctional alkane derivative [8,37].

The fragmentation pattern upon dissociative ionization of 3-methyl valeramide **1** parallels that of the parent compound valeramide, where some minor differences in the low-abundant CH_3-, C_2H_4-, C_2H_5- and C_3H_7-losses are readily explained by the change in the alkyl skeleton. The changes occurring in the "McLafferty region", however, bear greater significance and are way more delicate in nature as far as a quantitative analysis is concerned. Specifically, the methyl group introduced as a diastereotopic marker at C(3) provides an additional site for the McLafferty rearrangement. Moreover, the occurrence of a double-hydrogen transfer renders the analysis of the product distribution even more difficult. Only a comprehensive kinetic modeling can therefore provide the relevant rate constants, isotope effects, and finally the steric effect at all studied photon energies [25].

The steric effect of the McLafferty reaction at C(4) is quite pronounced and surprisingly decreases with the internal energy content of the ionized amide. This phenomenon can be attributed to the lifetime of the ion-neutral complex **2**/**3**$^{+\bullet}$. At high $E_{h\nu}$, dissociation into butene and $H_2C{=}C(OH)NH_2{}^{+\bullet}$ occurs almost instantaneously, whereas the complex has a distinctly longer lifetime when formed close to the threshold of dissociative photoionization. As a consequence, not only subsequent rearrangement as in the course of [McLafferty + 1] can take place, but partial equilibration of the intermediates can also result in a loss of stereochemical information, thus leading to a decrease of diastereoselective discrimination at low photon energies [38].

Acknowledgments

Financial support by the Deutsche Forschungsgemeinschaft, the Fonds der Chemischen Industrie, and the Gesellschaft von Freunden der Technischen Universität Berlin is gratefully acknowledged. We are indebted to C. Alcaraz and the entire staff of LURE, Orsay, for helpful assistance in the photoionization experiments using synchrotron radiation, and thank A. Chabane and J.-F. Bernadac for their cooperation. DS thanks the Laboratoire Chimie-Physique at Orsay for a visiting professorship which initiated this collaboration. Very special thanks are due to Dr. Marija Semialjac-Süßkind, who kindly provided some complementary B3LYP data.

Appendix A. Procedure of the kinetic modeling

As detailed in the text, 3-methyl valeramide (**1**) undergoes four different McLafferty-type reactions, of which some products are isobaric or even identical in elemental composition. For a decisive analysis of the regiochemistry, the isotopomers **1**–**1e** were examined (at photon energies of 9.6, 10, and 11 eV, respectively). To model the signals within the McLafferty-product region for each isotopomer, a number of kinetic equations was used, employing all together eight variables, i.e., the normalized rate constants k_I, k_{II}, and $k_{C(4')}$, the kinetic isotope effects KIE_I, KIE_{II}, KIE_{sec}, and KIE_{+1}, and the steric effect SE (see text). Two slightly different kinetic models were considered, of which one assumes the [McLafferty + 1] process to occur regiospecifically ("allylic model"), and the other is based on a full equilibration of the H/D-atoms in the backbone ("statistical model"). For the sake of simplicity, the normalized ($\Sigma = 100$) intensities are characterized according to the isotopomer's number and the respective ion's mass, e.g., $\underline{a}59$ represents the relative intensities of $m/z = 59$ formed from **1a**$^{+\bullet}$; $\_59$ stands for $m/z = 59$ formed from unlabeled **1**$^{+\bullet}$.

General

$k_{C(4)} = 1 - k_{C(4')}$

$k_{eq} = k_{C(4)}/(1 + 1/SE)$

$k_{ax} = k_{eq}/SE$

Allylic

$\_59 = k_{C(4)} \times k_I + k_{C(4')} \times k_{II}$

$\_60 = k_{C(4)} \times (1 - k_I) + k_{C(4')} \times (1 - k_{II})$

$\underline{a}59 = (k_{ax} \times k_I)/KIE_{sec} + k_{C(4')} \times k_{II}$

$\underline{a}60 = (k_{eq} \times k_I)/KIE_I + (k_{ax} \times (1 - k_I))/KIE_{sec} + 0.5 \times k_{C(4')} \times (1 - k_{II})$

$\underline{a}61 = (k_{eq} \times (1 - k_I))/KIE_I + 0.5 \times (k_{C(4')} \times (1 - k_{II}))/KIE_{+1}$

$\underline{b}59 = (k_{eq} \times k_I)/KIE_{sec} + k_{C(4')} \times k_{II}$

$\underline{b}60 = (k_{ax} \times k_I)/KIE_I + (k_{eq} \times (1 - k_I))/KIE_{sec} + 0.5 \times k_{C(4')} \times (1 - k_{II})$

$\underline{b}61 = (k_{ax} \times (1 - k_I))/KIE_I + 0.5 \times (k_{C(4')} \times (1 - k_{II}))/KIE_{+1}$

$\underline{c}59 = k_{C(4')} \times k_{II}$

$\underline{c}60 = (k_{C(4)} \times k_I)/(KIE_I \times KIE_{sec})$

$\underline{c}61 = (k_{C(4)} \times (1 - k_I))/(KIE_I \times KIE_{sec}) + (k_{C(4')} \times (1 - k_{II}))/KIE_{+1}$

$\underline{d}59 = k_{C(4)} \times k_I$

$\underline{d}60 = 0.5 \times k_{C(4)} \times (1 - k_I) + (k_{C(4')} \times k_{II})/KIE_{II}^*$

$\underline{d}61 = 0.5 \times (k_{C(4)} \times (1 - k_I))/KIE_{+1} + (k_{C(4')} \times (1 - k_{II}))/KIE_{II}^*$

$\underline{e}59 = k_{C(4)} \times k_I + k_{C(4')} \times k_{II}$

$\underline{e}60 = 0.5 \times k_{C(4)} \times (1 - k_I) + k_{C(4')} \times (1 - k_{II})$

$\underline{e}61 = 0.5 \times (k_{C(4)} \times (1 - k_I))/KIE_{+1}$

Statistical

$\_59 = k_{C(4)} \times k_I + k_{C(4')} \times k_{II}$

$\_60 = k_{C(4)} \times (1 - k_I) + k_{C(4')} \times (1 - k_{II})$

$\underline{a}59 = k_{ax} \times k_I/KIE_{sec} + k_{C(4')} \times k_{II}$

$\underline{a}60 = k_{eq} \times k_I/KIE_I + 0.875 \times k_{ax} \times (1 - k_I)/KIE_{sec} + 0.875 \times k_{C(4')} \times (1 - k_{II})$

$\underline{a}61 = k_{eq}/KIE_I \times (1 - k_I) + 0.125 \times k_{ax} \times (1 - k_I)/(KIE_{sec} \times KIE_{+1}) + 0.125 \times k_{C(4')} \times (1 - k_{II})/KIE_{+1}$

$\underline{b}59 = k_{eq} \times k_I/KIE_{sec} + k_{C(4')} \times k_{II}$

$\underline{b}60 = k_{ax} \times k_I/KIE_I + 0.875 \times k_{eq} \times (1 - k_I)/KIE_{sec} + 0.875 \times k_{C(4')} \times (1 - k_{II})$

$\underline{b}61 = k_{ax}/KIE_I \times (1 - k_I) + 0.125 \times k_{eq} \times (1 - k_I)/(KIE_{sec} \times KIE_{+1}) + 0.125 \times k_{C(4')} \times (1 - k_{II})/KIE_{+1}$

$\underline{c}59 = k_{C(4')} \times k_{II}$

$\underline{c}60 = k_{C(4)} \times k_I/(KIE_I \times KIE_{sec}) + 0.75 \times k_{C(4')} \times (1 - k_{II})$

$\underline{c}61 = 0.875 \times k_{C(4)}/(KIE_I \times KIE_{sec}) \times (1 - k_I) + 0.25 \times k_{C(4')} \times (1 - k_{II})/KIE_{+1}$

$\underline{c}62 = 0.125 \times k_{C(4)}/(KIE_I \times KIE_{sec} \times KIE_{+1}) \times (1 - k_I)$

$\underline{d}59 = k_{C(4)} \times k_I$

$\underline{d}60 = k_{C(4')} \times k_{II}/KIE_{II}^* + 0.625 \times k_{C(4)} \times (1 - k_I)$

$\underline{d}61 = 0.75 \times k_{C(4')}/KIE_{II}^* \times (1 - k_{II}) + 0.375 \times k_{C(4)} \times (1 - k_I)/KIE_{+1}$

$\underline{d}62 = 0.25 \times k_{C(4')}/(KIE_{II}^* \times KIE_{+1}) \times (1 - k_{II})$

$\underline{e}59 = k_{C(4)} \times k_I + k_{C(4')} \times k_{II}$

$\underline{e}60 = 0.625 \times k_{C(4)} \times (1 - k_I) + 0.625 \times k_{C(4')} \times (1 - k_{II})$

$\underline{e}61 = 0.375 \times (k_{C(4)} \times (1 - k_I))/KIE_{+1} + 0.375 \times k_{C(4')} \times (1 - k_{II})/KIE_{+1}$

Further, some general remarks about the modeling need to be made. Owing to the low intensities of some signals and because of minor contributions within composite signals, an analytical solution may yield misleading and questionable results due to inappropriate weighting of the data. A numerical approach, aimed at finding solutions which describe all signals in reasonable agreement with their error bars given by experiment, is therefore considered as a better choice. Programs which solve multi-parameter equations in an iterative manner have proven very useful for such purposes [34], but are unfortunately not suited for a system as complex as 3-methyl valeramide. Several different combinations of parameters may equally lead to satisfactory results, and with the "black box"-character of an iteration routine one runs into danger to get stuck in a local minimum of the solution space without finding the global minimum. Even if coincidentally found, the global minimum is not necessarily an adequate solution from a chemical point of view. Therefore, all possible solutions for the system of equations within the error margins of the experiments need to be considered, followed by an assessment of their quality. To this end, an algorithm is used which varies all parameters within their respectively defined regimes (see below), and all possible permutations are subsequently inserted into the kinetic equations to compute the respective ion intensities. The chosen increments for the parameter variations are 0.1 for the kinetic parameters (KIEs and SE), and 0.01 for the normalized ($\Sigma = 1$) rate constants. If the deviation of the modeled from the experimental data is within the experimental error bars, the respective set of parameters is kept as a member of the solution space. Whenever a border defining the variation range of one of the parameters is "touched", that is when a permutation containing a border value is still in agreement with the experimental data within the allowed error bars, that very range is extended. For a full determination of the solution space, all parameters have to be "converged", i.e., their borders are not touched anymore. In order to reach convergence for the kinetic isotope effect associated with the minor [McLafferty + 1] pathway (KIE_{+1}) the upper range has to be set unreasonably high. For this particular, quite insensitive variable, the parameter estimation requires some further steps (Appendix C). Otherwise, each kinetic parameter is determined as the average of all its entries in the solution space, and the respective maximal deviation is taken as a measure of the associated error. The solution spaces obtained for the allylic model comprises 929, 5081, and 2015 entries at 9.6, 10, and 11 eV, respectively, while the statistical model yields 93906, 9408, and 7650 results at these photon energies.

Boundary conditions for the KIEs of the [1,5]-H shifts. A peculiarity of the system in question originates from the fact that the competing γ- and γ′-hydrogen shifts are subject to different KIEs. Thus, the branching ratio is not only given by the mere rate constant $k_{C(4')}$, but also by the differences between the KIEs of C(4)–D and C(4′)–D bond activations. The resulting dependence of these KIEs yields a multi-dimensional solution space, in that a change in one parameter may be compensated by others. The kinetic modeling of the main signals ($m/z = 59$ and 60) would then yield an infinite number of solutions. The additional consideration of the minor signals with $m/z = 61$ is not fully sufficient to circumvent parameter dependences in the solution space, as the errors are considerable. In order to avoid the floating of two quasi-dependent parameters within the experimental error, a careful analysis of the experimental data prior to the modeling is compulsory to derive appropriate boundary conditions for the KIEs. The γ-C and γ′-C-deuterated isotopomers **1a**–**1d** are therefore subjected to a qualitative analysis of their $m/z = 59{:}60$ ratios at all three photon energies studied with the aim of extracting information about the KIEs. The mandatory subtraction of the [McLafferty + 1] contribution within the respective $m/z = 60$ signals is achieved in a simplistic approach by taking the respective relative intensity of $m/z = 60$ from unlabeled **1** as a measure for the combined amount of [McLafferty + 1] products which is to be expected at the respective photon energy. For the labeled compounds, this amount will be shared between non-deuterated [McLafferty + 1] ions ($m/z = 60$) and deuterated ones ($m/z = 61$). For each of the γ-C and γ′-C-deuterated isotopomers the respective relative intensity of the [McLafferty + 1] reaction transferring a D-atom ($m/z = 61$) is subtracted from the relative intensity of all [McLafferty + 1] reactions ($m/z = 60$ from **1**) to estimate the amount of interference in $m/z = 60$ by undeuterated [McLafferty + 1] ions. It has to be stated clearly that this deconvolution of single and double hydrogen transfer is a crude approximation because it assumes the amount of double hydrogen transfer to be identical for deuterated and non-deuterated ions. In reality, operation of KIE_{+1} and the possible competition of all channels, of which some are affected by KIEs, questions this simplification. However, considering that the [McLafferty + 1] reaction is low in abundance, at least at 10 and 11 eV, and that these simplifications are only used in the derivation of the boundary conditions, but not in the actual modeling, the approach appears justified. The modeling equations are hence simplified for the isotopomers **1a**–**1d** by omitting the [McLafferty + 1] related terms and using the [McLafferty + 1]-corrected renormalized intensities. Appropriate transformations and insertions of the simplified equations yield KIE_I and KIE_{II} as functions of KIE_{sec}.

The visualization of these dependences in Fig. A.1 implies inverse values to be rather unlikely for any of the three KIEs. $KIE_{sec} < 1.05$ would cause KIE_I to be inverse (<0.9), while KIE_{II} would have to assume values >2 (for 9.6 eV even >3.7). A pronounced inverse KIE_I along with a sizable, normal KIE_{II} is opposing any chemical intuition, as it would imply dramatic energy differences between the two [1,5]-H shifts. Likewise, an inverse KIE_{II} can be ruled out, because in that case the primary effect at C(4) (KIE_I) would be $\gg 1$. An inverse KIE_I finally, may only be considered if close to unity; values <0.8 would again lead to a clearly inverse KIE_I at a large, normal KIE_{II} (>2.5).

This qualitative analysis allows for a strict limitation of the range for KIE_{sec}. Only values slightly larger than one are chemically meaningful, whereas lower or higher values

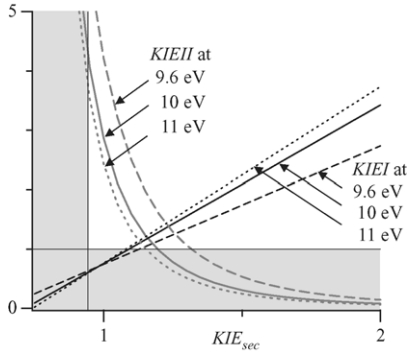

Fig. A.1. Dependences of KIE_I (black lines) and KIE_{II} (grey lines) on KIE_{sec} at photon energies 9.6 eV (dashed lines), 10 eV (solid lines), and 11 eV (dotted lines).

would cause the two primary KIEs of the [1,5]-H shift to display drastic differences in their respective order of magnitude. The range is in perfect agreement with the value derived for the respective secondary KIE of the unbranched valeramide, 1.07 ± 0.10, and we shall therefore adopt the very same value for the branched title compound. It is noted in passing that the necessity of $KIE_{sec} \geq 1.05$ (that means $\neq 1$) derived above clearly demonstrates the existence of the secondary KIE for the γ-H-shift.

Appendix B. Quality of the experimental data

Prerequisite for a kinetic modeling of experimentally observed intensity distributions is a critical inspection of the quality of the data. The mass spectra at 10 and 11 eV are highly reproducible, whereas those recorded at 9.6 eV have somewhat lower signal-to-noise ratios, owing to the proximity to the thresholds of dissociative photoionization.

A kinetic modeling should not exceed the accuracy of the experiment in order not to exclude chemically reasonable solutions which still agree with the experimental data within the error margins. As far as the experimental error margins are concerned, neither the assignment of a global absolute error nor of a global relative error appears justified [38]. Small peaks have smaller absolute errors than larger ones, so either one would be ill-estimated by the choice of a single value. In turn, the relative errors of small peaks are much higher than for large peaks, so again one can not chose a single value to cover all peaks. The obvious means to determine the experimental errors, the standard deviations derived from several spectra, would only be adequate if there were a significantly large number of spectra. Given the tight time schedule at a synchrotron facility, the various isotopomers to be examined, and the occurrence of significant memory effects, this approach was impossible, however. The data reported thus refer to the averages of only 2–4 independent experiments, which obviously does not suffice for a proper statistical error analysis. With the purpose of discounting points where the low number of events causes unreasonably low or high standard deviations, an appropriate error fit-function ΔI was derived from the standard deviations Δ in dependence of the intensities I of the whole ensemble of isotopomers. To this end, the plot of $\Delta(I)$ versus I was fitted by the arbitrary function $\Delta I(I) = (a + b \times (I - c)^d) \times I$. In order to achieve a stronger guidance for the parameters determining the slope of the fitting curve, a–d were chosen such that $\Delta I(I)/I = a + b \times (I - c)^d$ equally fitted the plot $\Delta(I)/I$ versus I. The fitting procedure was carried out for the data of all three photon energies, and the resulting values for a–d were 0.02, 0.033, −0.075, −1.4 at 9.6 eV, 0.003, 0.01, −0.015, −1.1 at 10 eV, and 0.003, 0.01, −0.01, −1.0 at 11 eV, respectively.

Appendix C. Modeling of the experimental intensities

As detailed in the text, the most plausible mechanism for the [McLafferty + 1] processes is a preferred participation of an allylic hydrogen from the intermediary butene moiety in the second H-transfer. To judge upon the importance of possibly accompanying minor H/D equilibrations, the modeling of an exclusively allylic scenario is completed by an independent modeling involving a completely statistical contribution of all butene hydrogens (resulting parameters listed in Table 3).

Estimation of KIE_{+1}. The low intensities of the [McLafferty + 1] channels not only render the elucidation of the underlying mechanism more difficult, but also hamper the determination of the associated KIE_{+1}. Specifically, the upper limit in the modeling has to be extended to unreasonably large values until convergence is reached (in one case even to $KIE_{+1} = 18.8$). The other parameters are not affected by KIE_{+1} within its upper range. Averaging of the solution space as for the other parameters is considered inappropriate because it would overestimate KIE_{+1} of the low abundance [McLafferty + 1] processes.

As an alternative approach for the estimation of KIE_{+1}, let us consider the isotopomers **1** and **1e**, which give the "purest" [McLafferty + 1] peaks, i.e., without overlap from deuterium transfer due to McL_I or McL_{II} reaction. Both $\mathbf{1}^{+\bullet}$ and $\mathbf{1e}^{+\bullet}$ form ions with $m/z = 59$ exclusively via McLafferty rearrangements, whereas $m/z = 60$ and 61 are due to [McLafferty + 1] reactions; KIE_{+1} is operative in the formation of $m/z = 61$ from $\mathbf{1e}^{+\bullet}$. According to the kinetic equations given in Appendix A, the exact dependence is given by Eq. (A.1.1) for the allylic model

$$KIE_{+1} = [0.5 \times k_{C(4)} \times (1 - k_I)]/\underline{e}61 \quad (A.1.1)$$

and by Eq. (A.1.2) for the statistical model

$$KIE_{+1} = 0.375 \times [k_{C(4)} \times (1 - k_I) + k_{C(4')} \times (1 - k_{II})]/\underline{e}61 \quad (A.1.2)$$

Calculation of the unknown terms in square brackets is possible by renormalizing the intensities of **1e** to $\underline{e}59 = \_59$. In the allylic model, the term in square brackets (Eq. (A.1.1) can

Table A.1
Intensities[a] of the McLafferty-related channels for $\mathbf{1}^{+\bullet}$ and its isotopomers derived from kinetic modeling[b] for the allylic model

$E_{h\nu}$	9.6 eV			10 eV			11 eV		
	59	60	61	59	60	61	59	60	61
1	849/−38	151/38		939/2	61/−2		970/1	30/−1	
1a	486/−39	469/−2	45/41	570/−2	398/−2	32/4	622/−9	361/7	17/3
1b	658/−25	307/−20	34/46	800/1	186/2	15/−3	848/−7	144/5	8/3
1c	301/10	617/5	82/−15	450/9	504/2	46/−12	513/−3	463/11	25/−8
1d	677/−1	228/27	95/−27	650/3	326/1	24/−3	613/−4	374/7	14/−3
1e	859/−15	134/−5	6/20	951/−1	42/1	7/−1	975/−1	20/2	5/−1

The deviations from the experimental data in Table 1 are given behind the dashes. Given as $\Delta I = I_{exp} - I_{mod}$. The average absolute deviation over all photon energies is ±10 (of 1000); the average relative deviation is 11%.

[a] Normalized to $\Sigma = 1000$.

[b] The non-rounded parameters resulting from averaging of the respective solution spaces were taken (Table 3). For KIE_{+1} at $E_{h\nu}$ = 9.6, 10, and 11 eV, the values 3, 3, and 2 were used.

Table A.2
Intensities[a] of the McLafferty-related channels for $\mathbf{1}^{+\bullet}$ and its isotopomers derived from kinetic modeling[b] for the statistical model

$E_{h\nu}$	9.6 eV				10 eV				11 eV			
	59	60	61	62	59	60	61	62	59	60	61	62
1	823/−12	177/12			934/7	67/−7			970/1	30/−1		
1a	469/−23	452/14	78/9		563/6	404/−8	34/2		621/−9	364/4	15/5	
1b	629/4	324/−37	47/33		797/3	188/−1	15/−3		847/−7	146/3	7/4	
1c	294/18	598/24	104/−37	5/−5	447/12	512/−6	39/−5	1/−1	512/−2	469/4	18/−1	1/−1
1d	684/−7	264/−9	49/20	3/−3	648/5	334/−8	17/4	1/−1	614/−6	377/4	9/2	1/−1
1e	861/−17	116/14	23/3		951/−1	42/1	6/−1		977/−4	19/3	4/1	

The deviations from the experimental data in Table 1 are given behind the dashes. Given as $\Delta I = I_{exp} - I_{mod}$. The average absolute deviation over all photon energies is ±6 (of 1000); the average relative deviation is 18%.

[a] Normalized to $\Sigma = 1000$.

[b] The non-rounded parameters resulting from averaging of the respective solution spaces were taken (Table 3). For KIE_{+1} at $E_{h\nu}$ = 9.6, 10, and 11 eV, the values 3, 4, and 3 were used.

equally be expressed by the difference between the intensities of $m/z = 60$ from both isotopomers, **1** and **1e** (_60–e60):

$$[0.5 \times k_{C(4)} \times (1 - k_I)] = \_60 - e60 \quad \text{(A.2.1)}$$

For the statistical case, the term in square brackets (Eq. (A.1.2) can equally be obtained by two independent approaches, one using the renormalized intensity of $m/z = 60$ from **1e** (e60), the other employing the intensity of $m/z = 60$ from **1** (60):

$$[k_{C(4)} \times (1 - k_I) + k_{C(4')} \times (1 - k_{II})] = e60/0.625 \quad \text{(A.2.2a)}$$

$$[k_{C(4)} \times (1 - k_I) + k_{C(4')} \times (1 - k_{II})] = \_60 \quad \text{(A.2.2b)}$$

The values of KIE_{+1} resulting from insertions of Eqs. (A.2.1) in (A.1.1) and (2.2) in (1.2) for $E_{h\nu}$ = 9.6, 10, and 11 eV, respectively, are listed in Table 3; for the statistical approach, the average values resulting from Eqs. (A.2.2a) and (A.2.2b) are given. Considering the error (±2), KIE_{+1} can be regarded as ∼3 independently of $E_{h\nu}$ or model.

Modeled intensities. In order to avoid numerical errors in the kinetic modeling, the ion intensities were included with one digit more than given in Table 1 of the text. Tables A.1 and A.2 list the modeled intensities and their deviations from the experiment, where the fragments are normalized to $\Sigma = 1000$.

The intensities resulting from the modeled parameters are given in Tables A.1 and A.2. The error margins of the modeling results are moderate, especially for the more intense data obtained at $E_{h\nu}$ = 10 and 11 eV. The average of the absolute deviations $|I_{exp} - I_{mod}|$ is slightly lower for the statistical modeling than for the allylic, while the average of the relative deviations $|(I_{exp} - I_{mod})/I_{exp}|$ is slightly larger for the statistical modeling than for the allylic. It is noted in passing that this opposing tendency in the error comportment underlines again the insufficiency of either error-determination method (absolute and relative) to describe the error margins of signals with very different magnitudes.

Even for a full equilibration between the butene hydrogens in the statistical model, the expected relative abundances for $m/z = 62$ for isotopomers **1c** and **1d** would not exceed 5‰. Hence, an only partial equilibration would be below the detection limits of the experiment and may well accompany the allylic H-shift. At any rate, the parameter analysis clearly demonstrates the insignificance of the differences between both models. It is therefore not only impossible, but also not required to determine the exact degree of equilibration in the minuscule [McLafferty + 1] reactions.

References

[1] F.W. McLafferty, Anal. Chem. 28 (1956) 306.
[2] F.W. McLafferty, Anal. Chem. 31 (1959) 82.
[3] (a) J. Loos, D. Schröder, H. Schwarz, in: N.M.M. Nibbering (Ed.), Encyclopedia of Mass Spectrometry, vol. 4, Elsevier, Amsterdam, in press;
(b) T. Weiske, H. Schwarz, Tetrahedron 42 (1986) 6245.
[4] G. Eadon, Org. Mass Spectrom. 12 (1977) 671.
[5] H.-E. Audier, H. Felkin, M. Fetizon, W. Vetter, Bull. Soc. Chim. Fr. 11 (1965) 3236.
[6] M.M. Green, R.J. McCluskey, J. Vogt, J. Am. Chem. Soc. 104 (1982) 2262.
[7] K. Zhang, S. Bouchonnet, S.V. Serafin, T.H. Morton, Int. J. Mass Spectrom. 227 (2003) 175, and references therein.
[8] D. Schröder, H. Schwarz, Top. Curr. Chem. 225 (2003) 133.
[9] D. Kreft, H.F. Grützmacher, Eur. J. Mass Spectrom. 4 (1998) 63.
[10] J. Loos, D. Schröder, W. Zummack, H. Schwarz, R. Thissen, O. Dutuit, Int. J. Mass Spectrom. 214 (2002) 105.
[11] M. Semialjac, J. Loos, D. Schröder, H. Schwarz, Int. J. Mass Spectrom. 214 (2002) 129.
[12] D. Schröder, J. Loos, M. Semialjac, T. Weiske, H. Schwarz, G. Höhne, R. Thissen, O. Dutuit, Int. J. Mass Spectrom. 214 (2002) 155.
[13] M. Semialjac, D. Schröder, H. Schwarz, Chem. Eur. J. 9 (2003) 4396.
[14] O. Dutuit, C. Alcaraz, D. Gerlich, P.M. Guyon, J.W. Hepburn, C. Metayer-Zeitoun, J.B. Ozenne, T. Weng, Chem. Phys. 209 (1996) 177.
[15] D. Schröder, H. Schwarz, J. Am. Chem. Soc. 112 (1990) 5947;
(b) G. Hornung, Dissertation, TU Berlin D83, 1998 (©dissertation.de, Berlin, Germany, 1998. Copies can be downloaded from http://www.dissertation.de).
[16] G. Hornung, D. Schröder, H. Schwarz, J. Am. Chem. Soc. 117 (1995) 8192.
[17] K. Watanabe, T. Nakayama, J. Mottl, J. Quant. Spectrosc. Radiat. Transfer 2 (1962) 369.
[18] F.W. McLafferty, F. Tureček (Eds.), Interpretation of Mass Spectra, 4th ed., University Science Books, Mill Valley, 1993, p. 81ff.
[19] G. Spiteller (Ed.), Massenspektrometrische Strukturanalyse Organischer Verbindungen, Verlag Chemie, Weinheim, 1966, p. 127.
[20] W. Carpenter, A.M. Duffield, C. Djerassi, J. Am. Chem. Soc. 90 (1968) 160.
[21] N.C. Rol, Rec. Trav. Chim. 84 (1965) 413.
[22] C. Djerassi, C. Fenselau, J. Am. Chem. Soc. 87 (1965) 5756.
[23] W. Carpenter, A.M. Duffield, C. Djerassi, J. Am. Chem. Soc. 89 (1967) 6164.
[24] M.B. Stringer, D.J. Underwood, J.H. Bowie, C.E. Allison, K.F. Donchi, P.J. Derrick, Org. Mass Spectrom. 27 (1992) 270.
[25] J. Loos, D. Schröder, H. Schwarz, J. Org. Chem., submitted for publication.
[26] M.B. Smith, J. March (Eds.), March's Advanced Organic Chemistry, Wiley/Interscience, New York, 2001, p. 243.
[27] (a) M.J. Frisch, K. Raghavachari, J.A. Pople, W.J. Bouma, L. Radom, Chem. Phys. 75 (1983) 323;
(b) B.F. Yates, R.H. Nobes, L. Radom, Chem. Phys. Lett. 116 (1985) 474;
(c) N. Heinrich, H. Schwarz, in: J.P. Maier (Ed.), Ion and Cluster-ion Spectroscopy and Structure, Elsevier, Amsterdam, 1989, p. 329.
[28] S. Hammerum, in: K.R. Jennings (Ed.), Fundamentals of Gas Phase Ion Chemistry, Kluwer Academic Publishers, Dordrecht, 1990, p. 379, and references therein.
[29] D.J. McAdoo, C.E. Hudson, M. Skyiepal, E. Broido, L.L. Griffin, J. Am. Chem. Soc. 109 (1987) 7648.
[30] S. Dohmeier-Fischer, N. Krämer, H.F. Grützmacher, Eur. J. Mass Spectrom. 1 (1995) 3.
[31] P. Mourgues, C. Monteiro, H.-E. Audier, S. Hammerum, Org. Mass Spectrom. 25 (1990) 389.
[32] R. Weber, K. Levsen, C. Wesdemiotis, T. Weiske, H. Schwarz, Int. J. Mass Spectrom. Ion Phys. 43 (1982) 131.
[33] A. Thibblin, P. Ahlberg, Chem. Soc. Rev. 18 (1989) 209.
[34] (a) C. Trage, W. Zummack, D. Schröder, H. Schwarz, Angew. Chem. 113 (2001) 2780;
(b) C. Trage, W. Zummack, D. Schröder, H. Schwarz, Angew. Chem. Int. Ed. Engl. 40 (2001) 2708;
(c) C. Trage, D. Schröder, H. Schwarz, Organometallics 22 (2003) 693.
[35] D. Schröder, H. Schwarz, Int. J. Mass Spectrom. 231 (2004) 139.
[36] (a) T. Prüsse, A. Fiedler, H. Schwarz, Helv. Chim. Acta 74 (1991) 1127;
(b) T. Prüsse, Dissertation, TU Berlin D83, 1991.
[37] J.S. Splitter, in: J.S. Splitter, F. Tureček (Eds.), Applications of Mass Spectrometry to Organic Stereochemistry, Verlag Chemie, Weinheim, 1994, p. 83.
[38] D. Schröder, H. Schwarz, J. Organomet. Chem. 504 (1995) 123.